Energy Transfer to Resonant Zonal Rossby Modes in Two-Dimensional Turbulence on a Rotating Sphere

Kiori Obuse[1]* and Michio Yamada[2]

[1]*Graduate School of Environmental and Life Science, Okayama University, Okayama 700-8530, Japan*

[2]*Research Institute for Mathematical Sciences, Kyoto University, Kyoto 606-8502, Japan*

The transfer of energy by the nonlinear interaction of Rossby waves in two-dimensional turbulence on a rotating sphere was investigated in this study. Although it has been suggested that three-wave resonant interaction dominates nonlinear interactions when the rotation rate of the sphere is sufficiently high, resonant interactions do not transfer energy to zonal Rossby waves, resulting in the nonresonant interaction of Rossby waves being responsible for the generation of zonal flows (G.M. Reznik, L.I. Piterbarg, and E.A. Kartashova, *Dyn. Atoms. Oceans* **18**, 1993; K. Obuse and M. Yamada, *Phys. Rev. Fluids* **4**, 2019). The resonant and nonresonant interactions of Rossby waves were investigated in this study, and it was found that although energy is transferred to the zonal Rossby modes by the nonresonant three-wave interaction of Rossby waves, the target of this nonresonant energy transfer is only the *resonant* zonal Rossby waves.

1. Introduction

Two-dimensional turbulence on a plane has long been studied, and there exist many detailed discussions on this topic in the literature.[1,2)] However, two-dimensional turbulence on other geometries has not been fully investigated. It is known that strong westward circumpolar flows are formed on a rotating sphere because of an effect arising from the rotation.[3)] This is probably the most simple example of anisotropic and inhomogeneous turbulence, yet even in this case, the mechanism responsible for the formation of zonal flows has still not been made clear. Much work has been done on zonal flow formations in two-dimensional turbulence on a rotating sphere from various

*obuse@okayama-u.ac.jp

points of view, such as the momentum dissipation of Rossby waves at critical layers[4–7] and the existence of a quasi-invariant quantity called zonostrophy[8]

The three-wave resonant and nonresonant nonlinear interactions of Rossby waves is one phenomenon often considered in the investigation of the mechanisms of zonal flow formation. The basic properties of resonant and nonresonant nonlinear interactions of Rossby waves on a β-plane have been investigated in the past.[9–11]

It should be noted that discussion on and knowledge of resonant and nonresonant interactions on a β-plane cannot be directly applied to the case of a rotating sphere. It is known that resonant interaction is the dominant part of the nonlinear interaction of Rossby waves when the rotation effect is sufficiently large, both on a β-plane[12] and a rotating sphere.[13] On a β-plane, resonant interactions that contain at least one zonal Rossby mode, which we define to be the Rossby wave independent of the longitudinal coordinate, are known to have no effect on the temporal variation of the flow field. In other words, the nonlinear terms corresponding to such resonant interactions completely vanish. In spherical geometry, however, some resonant triads that contain a zonal Rossby mode survive and change the phases of the Rossby modes participating in the resonant interactions while the energy of each mode is kept invariant. Thus, resonant interactions including zonal Rossby modes do not exchange any energy among the Rossby modes therein[14–16] but exert a significant influence on the temporal development of the flow field.[16] This means that nonresonant interaction is an indispensable mechanism for zonal flow formation in this system.

Therefore in this study, to understand the mechanism of zonal flow formation in two-dimensional turbulence on a rotating sphere, the resonant and nonresonant nonlinear interactions of Rossby waves were investigated. For this purpose, all the Rossby waves were first classified into four sets based on whether they are zonal and whether there exists a resonant interaction that includes them. The energy exchange among the four sets of Rossby waves was then studied.

The remainder of this paper is organized as follows. Section 2 describes the numerical methods used in this study, and the results of the numerical experiments are presented in Section 3. Section 4 concludes the paper. The energy transfer between two Rossby modes is also discussed in detail in Appendix.

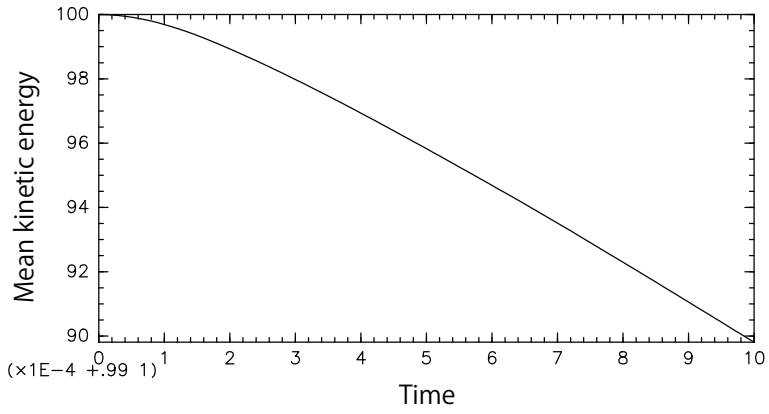

Fig. 1. Temporal development of the mean kinetic energy from $t = 0$ to $t = 10$ of the case $\nu_{2p} = 1.0 \times 10^{-38}$.

2. Equation of Motion and Numerical Methods

A nondimensionalized vorticity equation for a decaying two-dimensional barotropic incompressible flow on a rotating sphere was considered in this study. This equation is given as

$$\frac{\partial \zeta}{\partial t} + J(\psi, \zeta) + 2\Omega \frac{\partial \psi}{\partial \phi} = (-1)^{p+1} \nu_{2p} \left(\nabla^2 + 2\right)^p \zeta, \tag{1}$$

where $J(f, g)$ is the Jacobian operator, which is defined as $J(f, g) \equiv (\partial f/\partial\phi)(\partial g/\partial\mu) - (\partial f/\partial\mu)(\partial g/\partial\phi)$. Note that constant 2 is added in the viscosity term in order to conserve the total angular momentum of the system.[14)]

The explanation of variables, functions, and parameters is given in Table I, where ∇^2 is the horizontal Laplacian on a sphere. The dimensionless kinematic hyperviscosity coefficient was set to $\nu_{2p} = 0.0$ as a main case in this study to consider turbulence with an infinitely high Reynolds number. We have also considered of $\nu_{2p} = 1.0 \times 10^{-38}$ as a case where the viscosity term brings about very weak but significant viscosity effect. The order of the viscosity term in this case is $O(10^{-2})$ and is rather small, however since the rate of the energy decrease is also $O(10^{-2})$ as shown in Fig.1, we consider that the viscosity term brings about significant influence in the time development of the total flow field.

The length, velocity, and time variables were nondimensionalized with respect to the radius a of the sphere, the characteristic velocity amplitude U_0 of the initial state, and the advection time scale a/U_0, respectively.

For the calculation, a spherical harmonic spectral method was used. Then the stream

Table I. Variables, functions, and parameters in Eq.(1).

notation	name	value
ϕ	longitude	
μ	sine latitude	
t	time	
$\psi(\phi,\mu,t)$	stream function	
$\zeta(\phi,\mu,t)$	vorticity ($\equiv \nabla^2\psi$)	
Ω	dimensionless constant rotation rate of the sphere	10^4
p	hyperviscosity index	8
ν_{2p}	dimensionless kinematic hyperviscosity coefficient	$0.0, 1.0\times10^{-38}$

function ψ was expanded as

$$\psi(\phi,\mu,t) = \sum_{l=1}^{N_T}\sum_{m=-l}^{l} \psi_l^m(t) Y_l^m(\phi,\mu) \tag{2}$$

$$= \sum_{l=1}^{N_T}\sum_{m=-l}^{l} \psi_l^m(t) P_l^m(\mu)\exp(im\phi), \tag{3}$$

where $Y_l^m(\phi,\mu)$ are the spherical harmonics, $P_l^m(\mu)$ are the associated Legendre polynomials ($l \in \mathcal{N}$, $m \in \mathcal{Z}$, $-l \le m \le l$), and $\psi_l^m(t)$ are the expansion coefficients. Hereafter, $Y_l^m(\phi,\mu)$ is sometimes referred to as Y_l^m for the sake of brevity. The truncation wavenumber N_T and the spatial grid points in the longitudinal and latitudinal directions N_{lon}, N_{lat} were set to $N_T = 170$, $N_{lon} = 512$ and $N_{lat} = 256$, respectively. This eliminates aliasing errors. The linear terms in Eq.(1) were analytically treated by utilizing exponential functions. Time integration was performed using the fourth-order Runge–Kutta method with a time step of $\Delta t = 4\times10^{-5}$.

The initial energy distribution was set to

$$E(l,t=0) = \frac{Al^{\gamma/2}}{(l+l_0)^\gamma}, \quad l_0 = 50, \quad \gamma = 100, \ (l \ge 2) \tag{4}$$

where A is defined such that

$$\sum_{l=2}^{N_T} E(l,t=0) = 1.0, \tag{5}$$

and we set the expansion coefficients for $l = 1$ to be zero. Note that we set the peak of the initial energy distribution at low wavenumber here, as this study focuses on the formation of circumpolar zonal flows which is a phenomena occurring in low-wavenumber

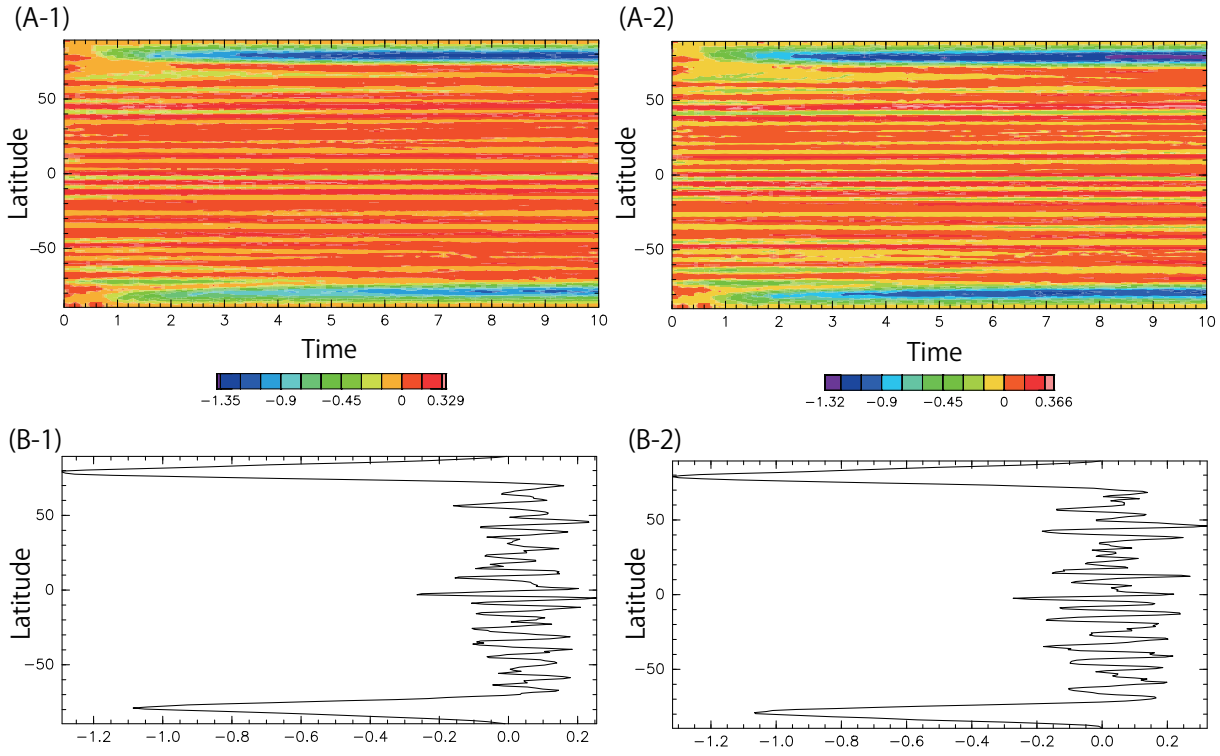

Fig. 2. (Color online) (A) Temporal development of the zonal-mean zonal angular momentum from $t = 0$ to $t = 10$. (B) Profile of the zonal-mean zonal angular momentum at $t = 10$. For both (A) and (B), (1) $\nu_{2p} = 0.0$ (2) $\nu_{2p} = 1.0 \times 10^{-38}$.

region.

Most of the settings described in this section were set essentially following Takehiro *et al.*[7)]

3. Energy Exchange by Nonlinear Terms

The temporal development of zonal jets, *i.e.*, the zonal-mean zonal angular momentum $\overline{[L_{lon}]}$, was first observed. Here, $\overline{[\cdots]}$ denotes the zonal mean, and $\overline{[L_{lon}]}$ is given by

$$\overline{[L_{lon}]} \equiv \frac{1}{2\pi}\int_0^{2\pi} u_{lon}\,\sqrt{1-\mu^2}\,\mathrm{d}\phi, \tag{6}$$

where $u_{lon} = -\sqrt{1-\mu^2}\,(\partial\psi/\partial\mu)$ is the longitudinal component of the velocity. Figure 2(A) shows the temporal development of the zonal-mean zonal angular momentum $\overline{[L_{lon}]}$ of inviscid and weak-viscosity cases from $t = 0$ to $t = 10$. In both the inviscid and the weak-viscosity cases, large-scale westward circumpolar zonal jets were formed, in accordance with results at larger viscosity coefficients obtained in previous studies.[3,7)] The profiles of the jets at a sufficiently large time ($t = 10$ here) are shown in Fig.2(B).

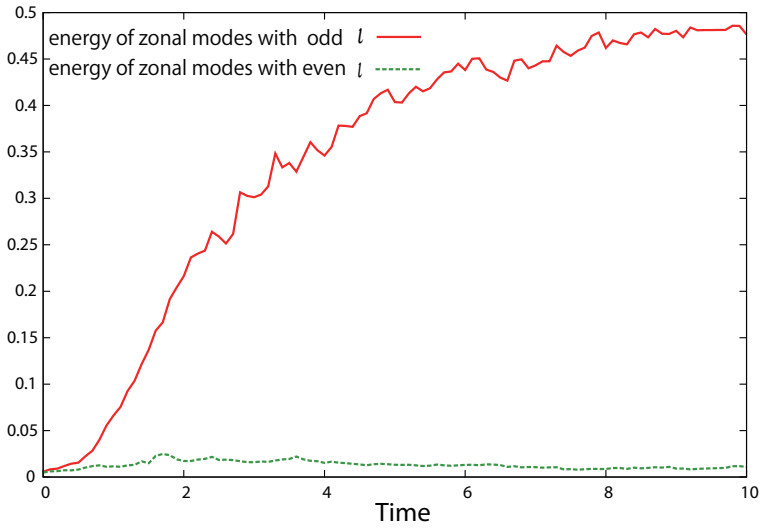

Fig. 3. (Color online) Temporal variation of the $Y^0_{l=odd}$ and $Y^0_{l=even}$ modes from $t = 0$ to $t = 10$ in $\nu_{2p} = 0.0$ case.

The formation of westward circumpolar zonal jets was also clearly observed in the energy spectra as the accumulation of energy in the zonal modes, *i.e.*, the Y^0_l modes (figure not shown). More precisely, from plots of the temporal variation of two types of zonal energy—the energy of Y^0_l with odd l modes and Y^0_l with even l modes—the formation of an equatorially symmetric zonal structure could be confirmed. Figure 3 shows the temporal variation in the energy of these two groups of modes, $Y^0_{l=odd}$ and $Y^0_{l=even}$ in the inviscid calculation. There is a strong energy accumulation in the $Y^0_{l=odd}$ modes, whereas the $Y^0_{l=even}$ modes gained little energy throughout the time integration. Because the $Y^0_{l=odd}$ modes correspond to equatorially symmetric zonal structures in a flow field, this is consistent with the formation of similar circumpolar zonal jets around both poles.

The energy accumulation in the $Y^0_{l=odd}$ modes in the energy spectrum may seem very natural at first glance if it is compared only with the numerical results for the formation of circumpolar zonal jets around both poles. However, the reason for the energy accumulation in the zonal modes, specifically only in $Y^0_{l=odd}$, is not understood at all. Moreover, this phenomenon is particularly noteworthy when considered from the viewpoint of nonlinear three-wave interactions.

The linear wave solutions of Eq.(1) are the Rossby waves $Y^m_l(\phi, \mu) \exp(i\omega t)$, and

the frequency ω of each wave is given as

$$\omega = \frac{-2m\Omega}{l(l+1)}. \tag{7}$$

In this paper, the Rossby waves are sometimes called "the Rossby modes" or simply "modes."

We then shifted our focus to the nonlinear three-wave interactions of Rossby waves. Nonlinear three-wave interactions can be classified as resonant or nonresonant interactions. Three Rossby waves $Y_{l_1}^{m_1}\exp(i\omega_1 t)$, $Y_{l_2}^{m_2}\exp(i\omega_2 t)$, and $Y_{l_3}^{m_3}\exp(i\omega_3 t)$ are said to undergo a resonant nonlinear three-wave interaction if the following conditions are satisfied:

$$m_1 = m_2 + m_3, \tag{8}$$

$$|l_2 - l_3| < l_1 < l_2 + l_3, \tag{9}$$

$$l_1 + l_2 + l_3 = \text{odd}, \tag{10}$$

$$\frac{m_1}{l_1(l_1+1)} = \frac{m_2}{l_2(l_2+1)} + \frac{m_3}{l_3(l_3+1)}. \tag{11}$$

Conditions (8)–(10) were derived by Silberman[14] as necessary conditions for nonlinear three-wave interactions. Note that nonlinear three-wave interactions include both resonant and nonresonant nonlinear interactions in the three-wave set, *i.e.*, a triad. When the nonresonant interactions are eliminated, condition (11) should be taken into account together with conditions (8)–(10).[15] Therefore, conditions (8)–(11) can be taken as the necessary conditions for the resonant nonlinear interaction of three waves. The zonal modes $Y_{l=odd}^0$ satisfy conditions (8)–(11), whereas the modes $Y_{l=even}^0$ do not. Nevertheless, any triad including a zonal mode as one of its elements does not have nonzero energy transfer by resonant three-wave interaction within the triad.[14–16] Therefore, in this paper, all the Rossby modes are categorized into the following four sets:

Resonant nonzonal ($R\breve{Z}$) modes

$$\{Y_l^{m\neq 0} \mid \text{with (8)–(11)}\}, \tag{12}$$

Resonant zonal (RZ) modes

$$\{Y_l^0 \mid \text{with (8)–(11)}\}$$
$$= \{Y_l^0 \mid l = \text{odd integer}\}, \tag{13}$$

Nonresonant zonal ($\breve{R}Z$) modes

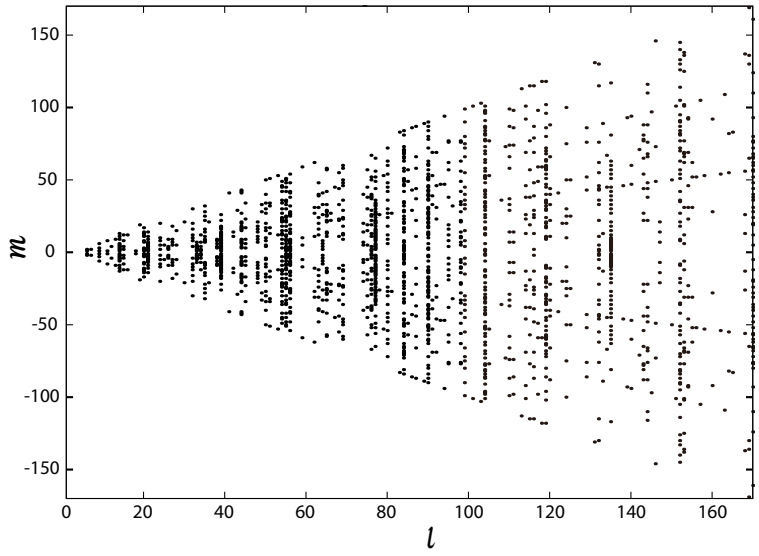

Fig. 4. $R\breve{Z}$ modes with $l \leq 170$.

$$\{Y_l^0 \mid l = \text{even integer}\}, \tag{14}$$

Nonresonant nonzonal ($\breve{R}\breve{Z}$) modes

$$\{\text{All Rossby modes}\} \setminus \{R\breve{Z}\} \setminus \{RZ\} \setminus \{\breve{R}Z\}, \tag{15}$$

where $\breve{A}$ means negation of A. The $R\breve{Z}$ modes with $l \leq 170$ are shown as dots in Fig.4. The numbers of elements in the four Rossby wave sets are $\#\{\breve{R}\breve{Z}\} = 26186$, $\#\{R\breve{Z}\} = 1684$, $\#\{\breve{R}Z\} = 86$, and $\#\{RZ\} = 85$ respectively in this case.

Let us return to the discussion of energy accumulation in the $Y^0_{l=odd}$ modes. Figure 5 shows the temporal development of the $R\breve{Z}$, RZ, $\breve{R}\breve{Z}$, and $\breve{R}Z$ modes in the inviscid and the weak-viscosity calculations. The RZ modes accumulate energy almost monotonically. The energy of the $\breve{R}\breve{Z}$ modes mostly decreases, whereas that of $R\breve{Z}$ gradually decreases after a slight initial increase.

The energy transfer among the four wave sets ($R\breve{Z}$, RZ, $\breve{R}\breve{Z}$, and $\breve{R}Z$) was then investigated. Because second-order nonlinear interaction is involved, the 10 possible combinations of the four wave sets must be considered, where a combination may contain the same set twice. Each of these 10 combinations transfers energy to the four wave sets, producing 40 cases in total.

The 40 nonlinear energy transfers were calculated after every five time steps of the numerical integration of Eq.(1), from $t = 2.0$ to 2.1 (2500 time steps), yielding a data set consisting of 500 time series of energy transfers. To calculate the energy transfer data at

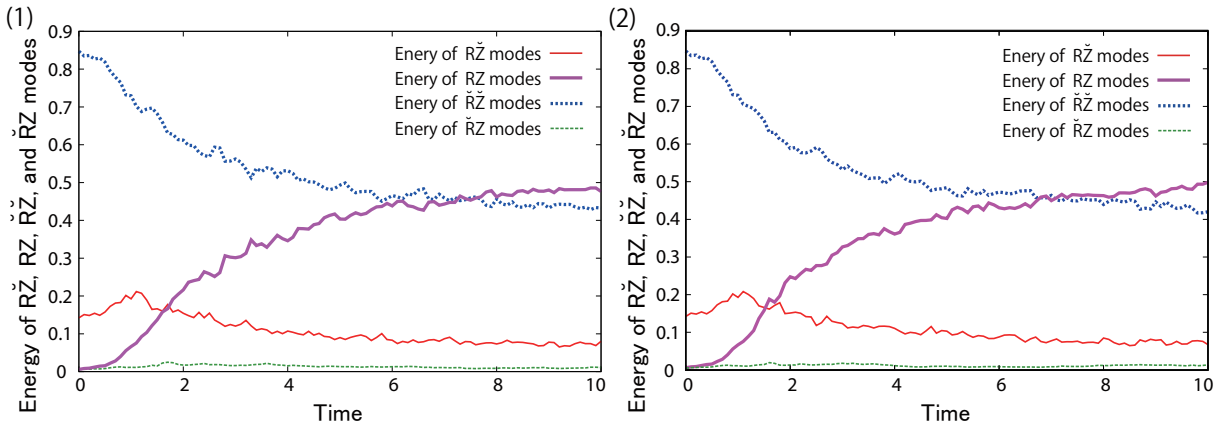

Fig. 5. (Color online) Temporal variation in the energy of the $R\check{Z}$, RZ, $\check{R}\check{Z}$, and $\check{R}Z$ modes from $t = 0$ to $t = 10$. (1) $\nu_{2p} = 0.0$ (2) $\nu_{2p} = 1.0 \times 10^{-38}$.

each time step, 10 filtered cases were first computed, corresponding to the 10 possible wave set combinations, which then yield the 40 nonlinear energy transfers though some algebraic manipulation. The 40 energy transfers were calculated for a relatively short time interval because the calculation requires the storage of a large amount of data. Figure 6 shows examples of nonlinear energy transfers to certain wave sets in the inviscid calculation, with standard deviations of the data set of 500 energy transfers, represented as error bars. Here we only used 100 equidistant data points out of 500 time series data for clear presentation. Although the considered time interval is rather short, we find the temporal fluctuation of energy transfers larger than the standard deviation. Table II gives the as-obtained 40 mean energy transfers by nonlinear terms per time integration step in the inviscid calculation. For example, -2.6626×10^{-7} at $(\check{R}Z, \check{R}\check{Z} \times \check{R}\check{Z})$ is the mean energy transfer to $\check{R}Z$ by the nonlinear interaction $\check{R}\check{Z} \times \check{R}\check{Z}$. It should be commented that we have obtained essentially the same result with Table II in our viscous case (not shown), and this, together with Fig.2 and Fig.5, implies that regardless of the existence of viscosity, the energy transfer is dominated by transfer toward the resonant zonal modes by the nonresonant interactions of nonzonal waves ($\check{R}\check{Z} \times \check{R}\check{Z} \to RZ$, $R\check{Z} \times R\check{Z} \to RZ$, and $\check{R}\check{Z} \times R\check{Z} \to RZ$).

4. Conclusions

In this study, the transfer of energy by the nonlinear interaction of Rossby waves in two-dimensional turbulence on a rotating sphere was investigated. To more closely observe the process of zonal flow formation, each of the Rossby waves was classified into one of four sets based on whether it is zonal and whether there exists a resonant inter-

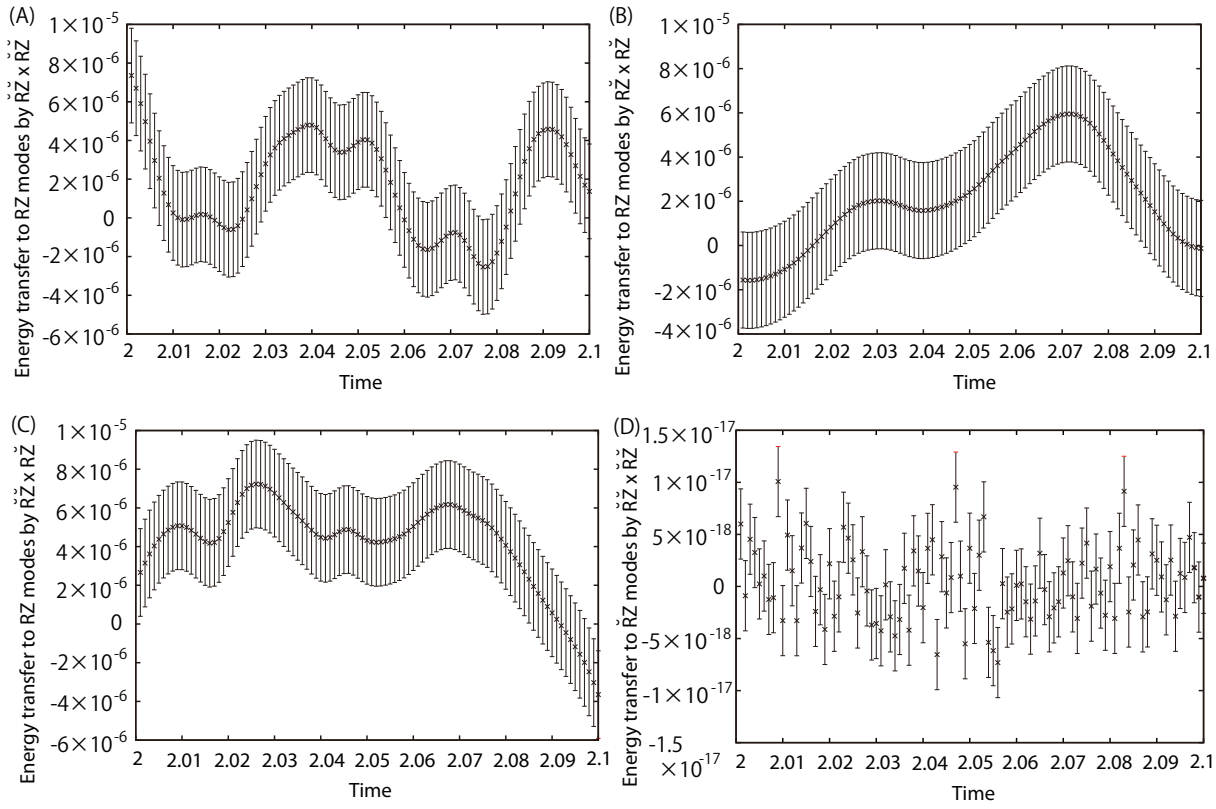

Fig. 6. Examples of energy transfer by nonlinear terms from $t = 2.0$ to $t = 2.1$ in $\nu_{2p} = 0.0$ case with standard deviations of the data set of 500 energy transfers, represented as error bars. (A) $\check{R}\check{Z} \times \check{R}\check{Z} \to RZ$. (B) $R\check{Z} \times R\check{Z} \to RZ$. (C) $\check{R}\check{Z} \times R\check{Z} \to RZ$. (D) $\check{R}\check{Z} \times \check{R}\check{Z} \to \check{R}Z$.

action that includes it. Then the energy exchange among the four sets of the Rossby waves was studied. It was demonstrated, that regardless of the presence of viscosity, energy accumulation occurs only in the *resonant* zonal modes, *i.e.,* zonal modes that satisfy the resonant three-wave interaction condition. It was also confirmed that there is high energy transfer to resonant zonal modes from nonzonal (resonant nonzonal and nonresonant nonzonal) modes by nonlinear three-wave interactions. This energy accumulation is all achieved by nonresonant three-wave interactions because the resonant zonal modes do not exchange energy with other modes by resonant interaction.[15,16] In the present system, although resonant zonal modes account for only 0.3% of the total number of Rossby waves, half of the total energy is concentrated in these modes because of the weak nonresonant interaction of Rossby waves. It should be stressed that this energy transfer results in the formation of a velocity profile symmetric about the equator. Asymmetric velocity profiles are realized only under external, likely asymmetric, forcing. For example, under random and uniform external forcing, multiple zonal-band

Table II. Mean energy transferred per time step among the $R\breve{Z}$, RZ, $\breve{R}\breve{Z}$, and $\breve{R}Z$ modes by nonlinear terms from $t = 2.0$ to $t = 2.1$ in $\nu_{2p} = 0.0$ case.

	$\breve{R}\breve{Z}$	$R\breve{Z}$	$\breve{R}Z$	RZ
$\breve{R}\breve{Z} \times \breve{R}\breve{Z}$	-9.9216×10^{-8}	1.2313×10^{-6}	-2.6626×10^{-7}	1.7378×10^{-6}
$R\breve{Z} \times R\breve{Z}$	1.2623×10^{-6}	-2.7770×10^{-8}	6.4728×10^{-7}	2.1270×10^{-6}
$\breve{R}Z \times \breve{R}Z$	0.0	0.0	-9.9341×10^{-20}	0.0
$RZ \times RZ$	0.0	0.0	0.0	0.0
$\breve{R}\breve{Z} \times R\breve{Z}$	-1.0387×10^{-6}	-1.3000×10^{-6}	-3.5807×10^{-7}	4.2133×10^{-6}
$\breve{R}\breve{Z} \times \breve{R}Z$	2.6761×10^{-7}	6.4791×10^{-7}	-7.8375×10^{-9}	-1.4854×10^{-9}
$\breve{R}\breve{Z} \times RZ$	-1.9167×10^{-6}	-1.4065×10^{-7}	-4.7346×10^{-10}	-1.9900×10^{-8}
$R\breve{Z} \times \breve{R}Z$	-2.7533×10^{-7}	-6.5265×10^{-7}	-2.7608×10^{-9}	-4.4679×10^{-10}
$R\breve{Z} \times RZ$	-3.8550×10^{-6}	-2.2587×10^{-6}	-2.7980×10^{-10}	-5.1366×10^{-9}
$\breve{R}Z \times RZ$	0.0	0.0	1.7710×10^{-19}	9.9563×10^{-19}
Total	-5.6438×10^{-6}	-2.4955×10^{-6}	1.1576×10^{-8}	8.0351×10^{-6}

structures are formed at first, then the structure tends toward two or three large zonal flows.[17,18)]

Acknowledgements

This work was supported by the Research Institute for Mathematical Sciences, an International Joint Usage/Research Center located in Kyoto University.

The first author is partially supported by the Program to Disseminate Tenure Tracking System, Ministry of Education, Culture, Sports, Science and Technology (MEXT), Japan, and the Japan Society for the Promotion of Science (JSPS) through KAKENHI Grant 17H02860. The second author is partially supported by JSPS through KAKENHI Grants 17H02860, 15K13458, and 24340016.

Some of the data analysis and visualizations in this paper were completed with ISPACK (http://www.gfd-dennou.org/library/ispack/index.htm.en), gt4f90io (http://www.gfd-dennou.org/library/gtool/index.htm.en), spmodel[19)] (http://www.gfd-dennou.org/library/spmodel/index.htm.en), and the software products of the GFD Dennou Ruby project (http://ruby.gfd-dennou.org/index.htm.en).

The numerical calculations were performed using the computer systems of the Research Institute for Mathematical Sciences, Kyoto University.

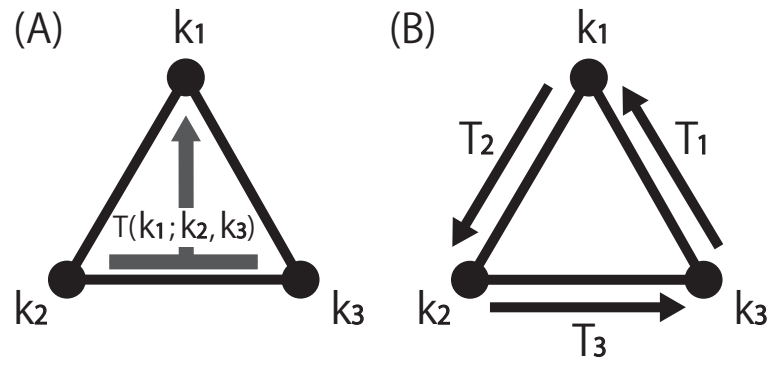

Fig. 7. (A) Nonlinear interaction triad and an energy transfer from two modes to the rest. (B) Effective energy transfer in a triad.

Appendix: Effective Energy Transfer Between Two Rossby Modes

The energy transferred from two Rossby modes to the rest of the modes in a nonlinear interaction triad (Figure 7(A)) is uniquely determined, but the energy transferred between two modes in such a triad is not uniquely determined in this system. Here, we define the effective energy transfer (EET) between two modes based on the detailed energy balance within a triad.

Consider a triad that consists of three modes whose wavenumbers are denoted $\mathbf{k_1}, \mathbf{k_2}$, and $\mathbf{k_3}$. The energy change of mode $\mathbf{k_i}$ ($i \in \{1, 2, 3\}$) caused only by nonlinear interactions within this triad is denoted E_i. Additionally, it is assumed that the EET from mode $\mathbf{k_{i-1}}$ to mode $\mathbf{k_i}$ in this triad is T_i (Figure 7(B)).

Then, the energy transferred within this triad is given by

$$\begin{pmatrix} E_1 \\ E_2 \\ E_3 \end{pmatrix} = \begin{pmatrix} 1 & -1 & 0 \\ 0 & 1 & -1 \\ -1 & 0 & 1 \end{pmatrix} \begin{pmatrix} T_1 \\ T_2 \\ T_3 \end{pmatrix} \tag{16}$$

$$= S \begin{pmatrix} T_1 \\ T_2 \\ T_3 \end{pmatrix}, \quad S \equiv \begin{pmatrix} 1 & -1 & 0 \\ 0 & 1 & -1 \\ -1 & 0 & 1 \end{pmatrix}. \tag{17}$$

The matrix S has three eigenvalues, 0 and $(3 \pm i\sqrt{3})/2$. For the case where the eigenvalue is zero, we obtain

$$\begin{aligned} T_1 - T_2 &= 0 \\ T_2 - T_3 &= 0 \\ T_3 - T_1 &= 0, \end{aligned} \tag{18}$$

yielding

$$T_1 = T_2 = T_3. \tag{19}$$

Now we recall that a detailed energy balance within this triad holds. This requires

$$T_1 + T_2 + T_3 = 0 \tag{20}$$

and thus excludes the uncertainty appearing in Eq.(19).

Then, from Eq.(16) together with Eq.(20), we obtain

$$\begin{pmatrix} T_1 \\ T_2 \\ T_3 \end{pmatrix} = \frac{1}{3} \begin{pmatrix} E_1 - E_3 \\ E_2 - E_1 \\ E_3 - E_2 \end{pmatrix}, \tag{21}$$

where the EET T_i is calculated from the information of the change in the energy of mode $\mathbf{k_i}$ caused only by nonlinear interactions in this triad. Then entire EET to mode $\mathbf{k_i}$ from mode $\mathbf{k_j}$ is obtained by summing T_i for all the possible triads, *i.e.*, considering all possible third modes.

Figure 8 shows examples of the EET at $t = 0.7$ in the numerical simulation shown in Fig.2(A-1) in Section 3. Fig.8(A) and (B) show examples of the EET from the nonresonant nonzonal modes, and Fig.8(C) and (D) show examples of the EET from the resonant nonzonal modes. In all cases, large EET values to resonant zonal modes ($Y_l^0, l =$ odd integer) were observed, whereas the EET to other modes was not large. This is consistent with the energy transferred between the four Rossby-mode sets discussed in Section 3 and suggests that the energy accumulation to zonal modes corresponding to circumpolar westward flow is achieved by the direct energy transfer to resonant zonal modes by nonresonant three-wave interactions.

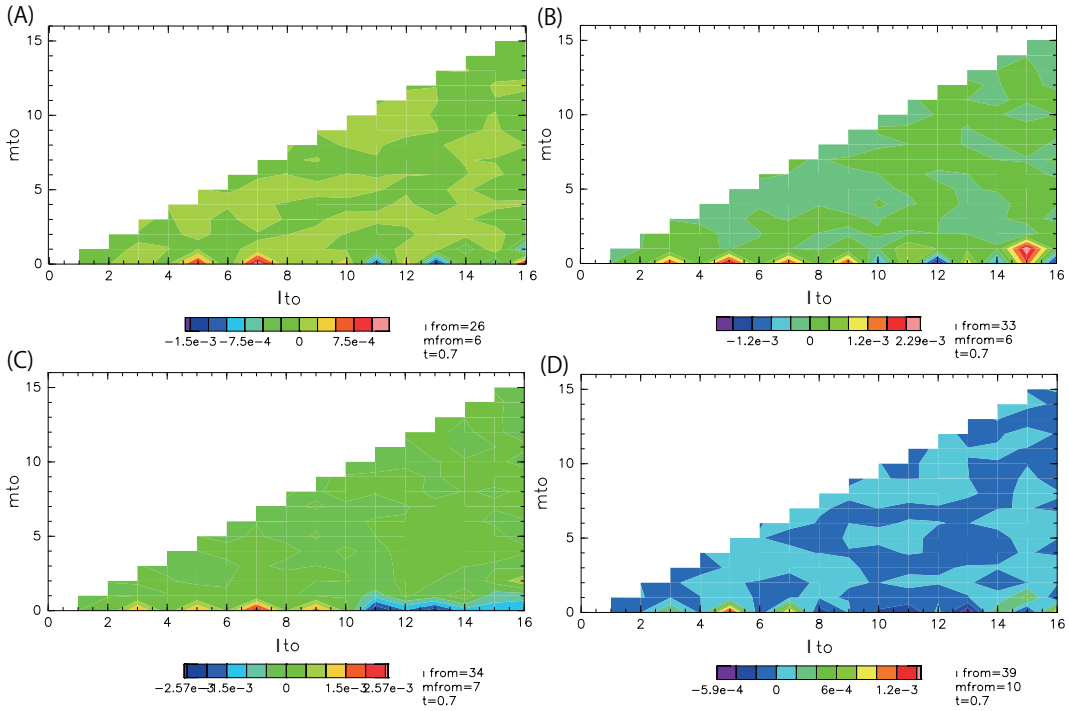

Fig. 8. (Color online) Examples of EET from mode $\mathbf{k}_{from} = (l_{from}, m_{from})$ to mode $\mathbf{k}_{to} = (l_{to}, m_{to})$. Only the range $0 \leq l_{to} \leq 16$, $-16 \leq m_{to} \leq 16$ is shown for simplicity. Examples of EET from nonresonant nonzonal modes with $\mathbf{k}_{from} = (l_{from}, m_{from}) =$ (A) $(26, 6)$ and (B) $(33, 6)$. Examples of EET from resonant nonzonal modes with $\mathbf{k}_{from} = (l_{from}, m_{from}) =$ (C) $(34, 7)$ and (D) $(39, 10)$.

References

1) U. Frisch, "Turbulence: The Legacy of A. N. Kolmogorov", Cambridge University Press, Cambridge, 1995

2) P. Davidson, "Turbulence: An Introduction for Scientists and Engineers"(2nd ed.), Oxford University Press, Oxford, 2015

3) S. Yoden and M. Yamada, "A numerical experiment on two-dimensional decaying turbulence on a rotating sphere", *J. Atomos. Sci.* **50**, 631–643 (1993)

4) G. Charney and P.G. Drazin, "Propagation of planetary-scale disturbances from the lower into the upper atmosphere", *J. Geophys. Res.* **66**, 83-110 (1961)

5) A. Eliassen and E. Palm, "On the transfer of energy in stationary mountain waves", *Geofys Publ.*, **22**, 1-23 (1961)

6) D.G. Andrews and M.E. McIntyre, "Planetary waves in horizontal and vertical shear: The generalized Eliassen-Palm relation and the mean zonal acceleration", *J. Atoms. Sci.*, **30**, 2031-2048 (1976)

7) S. Takehiro, M. Yamada, Y.-Y. Hayashi, "Energy accumulation in easterly circumpolar jets generated by two-dimensional barotropic decaying turbulence on a rapidly rotating sphere", *J. Atmos. Sci.* **64**, 4084–4097 (2007)

8) I. Saito and K. Ishioka, "On a quasi-invariant associated with the emergence of anisotropy in two-dimensional turbulence on a rotating sphere", *J. Meteor. Soc. Japan*, **94**, 25 — 39 (2016)

9) J. Sukhatme and L. M. Smith, "Local and nonlocal dispersive turbulence", *Phys. Fluids*, **21**, 056603 (2009)

10) A. M. Balk, "A new invariant for Rossby wave systems", *Phys. Lett. A*, **155**, 20-24 (1991)

11) S. Nazarenko and B. Quinn, "Triple cascade behavior in quasigeostrophic and drift turbulence and generation of zonal jets", *Phys. Rev. Lett.*, **103**, 118501, 2009

12) M. Yamada and T. Yoneda, "Resonant interaction of Rossby waves in two-dimensional flow on a β plane", *Physica D* **245**, 1–7 (2013)

13) A. Dutrifoy and M. Yamada, unpublished.

14) I. Silberman, "Planetary waves in the atmosphere", *J. Meteor.* **11**, 27–34 (1953)

15) G. M. Reznik, L.I. Piterbarg, and E.A. Kartashova, "Nonlinear interactions of spherical Rossby modes", *Dyn. Atoms. Oceans* **18**, 235–252 (1993)

16) K. Obuse and M. Yamada, "Three-wave resonant interactions and zonal flows in two-dimensional Rossby–Haurwitz wave turbulence on a rotating sphere", *Phys. Rev. Fluids* **4**, 024601 (2019)

17) T. Nozawa and S. Yoden, "Formation of zonal band structure in forced two-dimensional turbulence on a rotating sphere", *Phys. Fluids* **9**, 2081–2093 (1997)

18) K. Obuse, S. Takehiro, M. Yamada, "Long-time asymptotic states of forced two-dimensional barotropic incompressible flows on a rotating sphere", *Phys. Fluids.* **22**, 156601 (2010)

19) S. Takehiro, M. Odaka, K. Ishioka, M. Ishiwatari, Y.-Y. Hayashi, and SPMODEL Development Group, "A series of hierarchical spectral models for geophysical fluid dynamics", *Nagare Multimedia* (2006) Available on-line at: http://www.nagare.or.jp/mm/2006/spmodel/